Validation of a Mathematical Model Describing the Dynamics of Chemotherapy for Chronic Lymphocytic Leukemia In Vivo

Alessia Guadagnin Pattaro[1], Giovanni Plazzotta[1], Annarita Zanon[1]

Abstract
To be added

[1] *Master's degree in Quantitative and Computational Biology, University of Trento*

1. Introduction

The paper under analysis sets itself the aim of building a mathematical model able to describe the interaction between malignant chronic lymphocytic leukemia (CLL) cells, effector cells, which in the case of cancer response are mainly NK cells (innate immunity) and T CD8 lymphocytes (adaptive immunity). The dosage regimen reported in the paper uses two different drugs, the Bruton tyrosine kinase (BTK) inhibitor Ibrutinib (Ibr) and an inhibitor of the DNA polymerase enzyme, Cytarabine (Cyt), whose introduction has transformed CLL therapy and contributed to extend the overall survival of patients. Additional details about these small-molecule drugs will be presented in the sections below. While the formulation of a mathematical model describing the dynamics of cancer in an immunoactive environment is not innovative *per se*, this paper sets itself apart in the sense that:

- It deals with a blood cancer instead of a solid tumor: in blood cancers, cell growth, survival dynamics and cellular interactions within the tumor microenvironment likely differ considerably from solid tumors. It is expected that several parameters of previously formulated ODE-based computational models need to be adapted for blood-borne cancers.

- The majority of models use data generated by simulations to perform the parameter estimation, instead of experimental data. This paper, on the other hand, is strongly experimentally - oriented.

- When data are derived from experiments, these are often performed *in vitro* rather than *in vivo*, and many studies have demonstrated conflicting results, in particular for what concerns optimal drug doses, between these two approaches. This paper, on the other hand, describes *in vivo* experiments, performed on murine models injected with A20 CLL cells, aimed at the estimation of the cancer cells growth rate r and of the cytotoxicity rates μ_{AC} as a function of therapy.

1.1 Chronic Lymphocytic Leukemia

Chronic lymphocytic leukemia (CLL) is the most common type of blood cancer in adults in the Western world, with an incidence of 4.9 cases in 100000 people per year. It typically occurs in elderly patients, with the median age at diagnosis being 70 years. CLL is characterized by the clonal proliferation and accumulation of mature B lymphocytes in secondary lymphoid organs, spleen, peripheral blood, and bone marrow. [1, 2] There is no known cause for this disease, but it is suspected to have a genetic component. Loss or addition of large chromosomal material followed by additional mutations, that render the leukemia increasingly aggressive, are often observed. Additionally, mutations in *IGHV* (immunoglobulin heavy variable) genes distinguishing different types of clinical behaviours of CLL and are prognostic of patent outcome [3].

Different treatment strategies are available for patients suffering from CLL. It is important to notice that studies on early-stage disease were unable to show a benefit of early therapeutic interventions: treatment of patients with early stage CLL did not result in a survival benefit. For this reason, and not to fruitlessly trigger the development of drug resistance, patient in these stages should not be treated, but only monitored, until the disease becomes *active*. The degree of *activity* of CLL can be assessed using the following guidelines:

- Progressive lymphocytosis with an increase of $\geq 50\%$ over a 2 month period, or lymphocyte doubling time of less than 6 months.

- Worsening of anemia and/or thrombocytopenia

- Massive nodes (i.e., ≥ 10 cm in longest diameter)

- Massive or symptomatic splenomegaly and hepatomegaly

- Autoimmune complications

- Functional extranodal involvement (e.g., skin, kidney, lung, spine)

- Significant weight loss and fatigue, fevers above 38 degrees for more than two weeks, night sweats.

When the treatment becomes necessary, specialists can choose between different classes of drugs targeting different aspects of the cellular structure (e.g. surface antibodies), metabolism, and external microenvironment:

- **Cytostatic agents**: their goal is to stop cellular proliferation by interfering with the replication process. Examples are purine analogs, such as Cytarabine (Cyt), one of the two drugs that will be discussed in this presentation.

- **Monoclonal Antibodies**: specifically built to interact with surface antigens that have been documented to be overexpressed in malignancies, like CD-20 and CD-52 receptors in B-cells blood cancers. They have the goal of guiding the immune system towards the cancerous cells. Examples are Rituximab and Alemtuzumab.

- **Signalling-targeting agents**: having the goal of interfering with the embedded signalling pathways in order to trigger apoptosis. Ibrutinib (Ibr), the second drug discussed in this presentation, is a Bruton Tyrosine Kinase inhibitor that hinders the downstream propagation of the signal generated by bounded BCR receptors, stopping the activation of B cells survival pathways.

- **Immunotherapy**: different CART approaches are being explored.

Finally, a worth noting characteristics of CLL is its incurability, at least for the patients who do not undergo allogeneic stem cell transplantation. This is due to the very low level of clonality displayed by the majority of somatic *passenger* mutations that accumulate above the background of *driver* mutations that originally gave birth to the malignancy. A very low level of clonality implies a very high tumor heterogeneity, with different subpopulations carrying different sets of mutations, and in turn a very high tumor heterogeneity increases the probability of developing primary resistance.

2. Chemotherapeutic drugs

2.1 Ibrutinib (Ibr)

Ibrutinib (Ibr) is a chemotherapic drug (Fig. 1) used as a deactivator of Bruton tyrosine kinase (BTK). Whenever B cells receptor signaling has an aberrhant behaviour alongside antigen-dependent activation BTK is involved, this also includes the pathogenesis of many lymphocytes-related malignancies [4].

Ibr blocks B cell antigen receptor signalling through an irreversible covalent bond with Cys-481 of BTK, hence reducing malignant B cell proliferation and inducing cell death.

The drug reaches its maximum concentration in plasma (953 ng·h/mL at dosage of 560 mg/day) in 1-2 h and is widely distributed in the body. The major route of elimination is metabolism. It is metabolised by hepatic cytochrome P450 3A enzymes. It has an elimination half-life of 4-6 h via faeces.

It has been shown that Ibr has a high tolerance level in the body, clinical studies have shown that dose limiting events are not observed even with prolonged dosing [5] but saturation of the active site of BTK was reached after a single dose of 2.5 to 20 mg/kg [6]. Reported dosages administered Ibr in 1.25, 2.5, 5.0, 8.3, 12.5, and 17.5 mg/kg/day for 28 day orally, with a 7-day rest period [5].
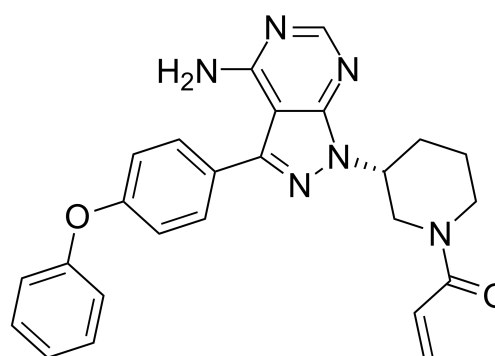
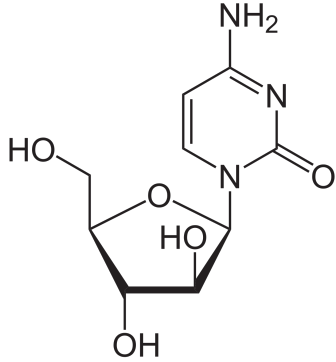**Figure 1.** Molecular structure of chemotherapeutic drug Ibrutinib

2.2 Cytarabine (Cyt)

Cytarabine (Cyt) is a medication used in treatment of leukemias and lymphomas. As it can be seen in Fig. 2, it is a nucleoside (pyrimidine analog) with arabinose sugar, also called arabinosylcytosine, and is an antimetabolite and antineoplastic. The sugar moiety induces the rotation of Cyt within the DNA, blocking DNA replication during the S-phase of cellular replication. It also acts on DNA polymerase and its maximum effects are seen after the time equivalent to a full cell cycle (8-12 h). The drug is admnistered via intravenous infusion and it was shown that the dose-response relationship for Cyt has a plateau above a dose level of 1000 mg/m^2 (intermediate dose). The reported dosage for patients is a first cycle with 200 mg/m^2 of Cyt infused continuously for 24 hours, and a second cycle with 1000 mg/m^2 infused for three hours twice a day [7]. Cyt has two types of metabolites:

- **inactive metabolites**, from deamination as soon as the drug enters the plasma

- **active metabolites** (Cyt triphosphate, CytTP), after being transported into the cell, and after phosphorylation.

The active metabolites competitively inhibit DNA polymerase, they are incorporated into DNA where they act as chain terminator, leading to incomplete DNA replication and cell death.

CytTP has a saturation level, leading to accumulation of the metabolite in cells, a lower drug selectivity of cancer cells, and a higher degree of myelosuppression.[8, 9]

Figure 2. Molecular structure of chemotherapeutic drug Cytarabine

3. Paper analysis

3.1 Mathematical model
Based on previous studies, an ODE model was formulated to explain the interaction between CLL cells, immune cells and chemotherapeutic drugs:

$$
\begin{cases}
\frac{dA}{dt} = rA\left(1 - \frac{A}{K}\right) - \mu_A AE - \frac{\mu_{AC} AC}{a+C} & (1) \\[2mm]
\frac{dE}{dt} = -\mu_E E + \frac{pAE}{c+A} - \mu_{AE} AE - \frac{\mu_{EC} EC}{b+C} & (2) \\[2mm]
\frac{dC}{dt} = \sum_{m=0}^{N-1} d\,\delta(t - m\tau) - \mu_C - \frac{\mu_{CA} CA}{a+A} & (3)
\end{cases}
$$

$\frac{dA}{dt}$ describes the dynamic of A20 mCherry cells. The first term reflects the assumption that cancer cells follow a logistic growth with *instantaneous growth rate r* and carrying capacity K. The carrying capacity represents the maximal tumor cell number that the system is able to host. A logistic growth is a reasonable assumption for cancer growth, since it takes place in a competitive environment with limited resources. Cancer cells can be killed by both NK cells (innate immunity) and T CD8 lymphocytes (adaptive immunity): these were considered together in the single variable E, whose dynamics is described in the second equation. The overall killing activity of immune cells can be modelled with the law of mass action, assuming a *killing efficiency μ_A*. The last term represents the effect of the treatment on tumor cells: the numerator simulates the interaction between tumor cells and drug molecules with the law of mass action, with a *killing efficiency μ_{AC}*, while the denominator introduces a Michaelis Menten drug saturation response, for which the whole term converges to the maximum killing rate $\mu_{AC} \cdot A$ as the drug concentration C is brought to infinity. This is reasonable strategy to model the drug response, since we expect a plateau in the effectiveness of

the drug as its concentration is increased. In this last term, a represents the drug concentration needed to reach half of the maximum killing rate.

$\frac{dE}{dt}$ describes the dynamic of immune effector cells. Their number is assumed to decline with rate μ_E due to natural death. It is known from literature that cancer cells are able to induce a recruitment effect on immune cells, due to the pro inflammatory environment defined by cancer itself. This is represented by the second term. The recruitment effect increases as the tumor mass grows, but up to a certain maximum rate, represented by $p \cdot E$. Additionally, c is the number of cancer cells by which the immune system response is half of its maximum. It is also known from literature that T CD8 and NK cells undergo apoptosis after a certain number of encounters with malignant cells: the cytotoxic molecules released against cancer inevitably cause damage to immune cells too, and this is modelled by the third term, using again the law of mass action. Finally, the drug administered to treat CLL also kills host immune cells: this is modelled as described above for cancer cells.

$\frac{dC}{dt}$ describes the first-order pharmacokinetics of a drug with an external source, with C being the concentration of the drug in the bloodstream. A dose d of the drug is injected every τ hours. By modeling the injection as a shifted Dirac Delta function $\delta(t - m\tau)$, the mth dose raises $C(t)$ by d units at $t = m\tau$. It was assumed that the drug was eliminated from the body with a rate μ_C, calculated as $\mu_C = \frac{\ln 2}{t_{1/2}}$, where $t_{1/2}$ is the elimination half-life of the drug (1–3 h for Cyt and 4–6 h for Ibr). The drug concentration can also be depleted by the interaction with cancer cells, having rate μ_{CA}. Finally, a represents the drug concentration producing 50% of the maximum activity in the A20 mCherry cell population.

3.2 Stability Analysis
3.2.1 Stability when $d = 0$, *i.e. without treatment*
The (1)-(3) model depends on time in the chemotherapy levels. Since equilibra cannot explicitly depend on t for each $t \in \mathbf{R}$, we can approximate $\sum_{m=0}^{N-1} d\delta(t - m\tau)$ using a uniform drug injection that takes the form $\frac{d}{\tau}$. The steady states are calculated by zeroing the gradient of the function, only non-negative equilibria are considered and all initial conditions are assumed to be positive. The absence of drug treatment has $d = 0$ and $C^* = 0$

$$
\begin{cases}
0 = rA\left(1 - \frac{A}{K}\right) - \mu_A AE - \frac{\mu_{AC} AC}{a+C} & (A1) \\[2mm]
0 = -\mu_E E + \frac{pAE}{c+A} - \mu_{AE} AE - \frac{\mu_{EC} EC}{b+C} & (A2) \\[2mm]
0 = \frac{d}{\tau} - \mu_C C - \frac{\mu_{CA} CA}{a+A} & (A3)
\end{cases}
$$

By applying the conditions for no treatment, the system

becomes

$$\begin{cases} 0 = rA\left(1 - \frac{A}{K}\right) - \mu_A AE - \cancel{\frac{\mu_{AC}AC}{a+C}}^{0} & (A1) \\ 0 = -\mu_E E + \frac{pAE}{c+A} - \mu_{AE}AE - \cancel{\frac{\mu_{EC}EC}{b+C}}^{0} & (A2) \\ 0 = \cancel{\frac{q}{\tau}}^{0} - \mu_C \cancel{C}^{0} - \cancel{\frac{\mu_{CA}CA}{a+A}}^{0} & (A3) \end{cases}$$

From Equation (A2) we find that $E^* = 0$, this cancels out the second term in Equation (A1),

$$\begin{cases} rA\left(1 - \frac{A}{K}\right) - \cancel{\mu_A AE}^{0} = 0 & (A1) \\ -\mu_E E + \frac{pAE}{c+A} - \mu_{AE}AE = 0 & (A2) \end{cases}$$

such that the following system is obtained

$$\begin{cases} rA\left(1 - \frac{A}{K}\right) = 0 & (A1) \\ E\left(-\mu_E + \frac{pA}{c+A} - \mu_{EA}A\right) = 0 & (A2) \end{cases}$$

Equation (A1) is a second-degree equation in A, where the first solution is $A_1^* = 0$ and the second is $A_2^* = K$. The part of Equation (A2) between parenthesis is now considered to find the other possible values of $A*$.

$$-\mu_E + \frac{pA}{c+A} - \mu_{EA}A = 0$$

$$-\mu_E(c+A) + pA - \mu_{EA}(c+A) = 0$$

$$c\mu_E - (p - \mu_E - c\mu_{EA}) \cdot A + \mu_{EA} \cdot A^2 = 0$$

The result is a second-degree equation, to find the solutions the usual discriminant formula can be employed. It is found that $A_3^* < 0$, which has no biological relevance, and $A_4^* = A_1^* = 0$. In conclusion, we have two equilibrium points:

$$Eq_0^* = \{A^* = 0, E^* = 0, C^* = 0\}$$

$$Eq_1^* = \{A^* = K, E^* = 0, C^* = 0\}$$

To study the stability of the equilibria of system (A1)-(A3), we need to compute the eigenvalues $\lambda = [\lambda_1, \lambda_2, \lambda_3]$ of the Jacobian matrix J

$$\mathbf{J} = \begin{bmatrix} \frac{\partial A1}{\partial A} & \frac{\partial A1}{\partial E} & \frac{\partial A1}{\partial C} \\ \frac{\partial A2}{\partial A} & \frac{\partial A2}{\partial E} & \frac{\partial A2}{\partial C} \\ \frac{\partial A3}{\partial A} & \frac{\partial A3}{\partial E} & \frac{\partial A3}{\partial C} \end{bmatrix}$$

For Eq_0^* we obtain

$$J = \begin{pmatrix} r & 0 & 0 \\ 0 & -\mu_E & 0 \\ 0 & 0 & -\mu_C \end{pmatrix}$$

that has eigenvalues $\lambda = [0.01, -4 \times 10^{-5}, -0.231]$ for Cyt and $\lambda = [0.01, -4 \times 10^{-5}, -0.116]$. For the equilibrium to be stable, all the (real parts) of the eigenvalues must be

negative. So Eq_0^* is NOT asymptotically stable.

For Eq_1^* we have

$$J = \begin{pmatrix} -r & -\mu_{AE}K & -\frac{\mu_{AC}K}{a} \\ 0 & -\mu_E + \frac{pK}{c+K} - \mu_{EA}K & 0 \\ 0 & 0 & -\mu_C - \frac{\mu_{CA}K}{a+K} \end{pmatrix}$$

which has eigenvalues $\lambda = [-0.01, -4 \times 10^{-5}, -0.35]$. So Eq_1^* is asymptotically stable.

3.3 Parameter estimation

Two parameters of the model, the ***in vivo* growth rate r of A20 mCherry cells** and the **cytotoxicity rate μ_{AC}** in the presence of drug, were experimentally derived with an *in vivo* approach, for which 20 murine models were considered.

To measure the instantaneous growth rate, 20 mice were inoculated with A20 murine leukemic cells. On day 16 after inoculation, blood was collected from the tail veins of four randomly chosen mice, and again on day 22 from four other mice. The proportion of A20 cells over the total was estimated using flow cytometry. Assuming a logistic growth (appropriate for cancer growth, since it takes place in a competitive environment with limited resources), we can compute the instantaneous growth rate as:

$$r = \frac{\ln N(t)/N(0)}{t} = \frac{\ln 16338/3662}{144} = 0.01 \ h^{-1}$$

Where $N(0), N(t)$ are the number of cells at times 0 (16 days after inoculation) and t (22 days, and so 144 hours, after inoculation).

For what concerns μ_{AC}, we notice that it's a crucial parameter for the model, since it represents the efficiency with whom a drug is able to kill cancer cells. Researchers were interested in computing μ_{AC}, by the means of *in vivo* experiments on murine model bearing the A20 cells, for the effect of two different drugs, Cytarabine (Cyt) and Ibrutinib (Ibr), in different doses. To apply the desired protocols, developed after reviewing the literature in which Cyt and Ibr had been used *in vivo*, researchers divided the 20 mice in 5 different groups:

1. Control group, which only received PBS.

2. Cyt Low group, which received 0.12 mg/kg of Cyt for 5 days. This is equivalent to injecting $5.94 \cdot 10^{15}$ molecules of Cyt at each administration.

3. Cyt High group, which received 62.5 mg/kg of Cyt for 3 days. This is equivalent to injecting $3 \cdot 10^{18}$ molecules of Cyt at each administration.

4. Ibr Low group, which received 9 mg/kg of Ibr in days 1-5 and 8-10. This is equivalent to injecting $2.5 \cdot 10^{17}$ molecules of Ibr at each administration.

5. Ibr High group, which received 18 mg/kg of Ibr on days 1–5 and 8–10. This is equivalent to injecting $5 \cdot 10^{17}$ molecules of Ibr at each administration.

To estimate μ_{AC} in groups 2 to 5, blood was collected from all mice, on the day of the initiation of the treatment and 2 days after the last treatment. At each of the two time points and in each treated mouse, the percent change in the frequency of A20 cells relative to the average frequency in the control group was calculated. Then, for each treated group, these individual measurements were then averaged. This led to the estimation of the *experimental cell growth inhibition percentage* for the 4 treated groups (Fig. 3).

Concentration of Drugs (mg/kg)
Cyt 0.12
Cyt 62.5
Ibr 9
Ibr 18
Cyt 62.5 + Ibr 9

Cell Growth Inhibition (%) from the Experiment Data
9
58
43.5
44.5
-

Figure 3. Drug dosages and resulting experimental cell growth inhibition percentage in the four treatment groups

We notice that growth inhibition due to Cyt was dose dependent, whereas inhibition due to Ibr was not. At this point, a total of 12 deterministic simulations were performed (Fig. 4), 3 for each treatment group, using $(A = 5.4 \cdot 10^4, E = 2500, C = 0)$ as starting point. In the context of the same treatment group, the simulations set themselves apart for the numerical choice of μ_{AC}: Cyt Low was tested with $\mu_{Ac} = 0.0001$, $\mu_{Ac} = 0.001$ and $\mu_{Ac} = 0.003$. Cyt High was tested with $\mu_{Ac} = 0.005$, $\mu_{Ac} = 0.012$, $\mu_{Ac} = 0.02$. Ibr Low was tested with $\mu_{Ac} = 0.001$, $\mu_{Ac} = 0.0041$, $\mu_{Ac} = 0.005$. Ibr High with $\mu_{Ac} = 0.002$, $\mu_{Ac} = 0.0042$, $\mu_{Ac} = 0.006$. Black lines represent cancer evolution without treatment. The goal was finding, for each treatment protocol, the value for μ_{Ac}, among the one proposed, that gives a *simulated cell growth inhibition percentage* similar for the one obtained from the experiments (Fig. 5).

- Cyt Low has a target cell growth inhibition percentage of 9%. This is best reached by using $\mu_{Ac} = 0.001$, that provided 10% of growth inhibition.

- Cyt High has a target cell growth inhibition percentage of 58%. This is best reached by using $\mu_{Ac} = 0.012$, that provided 59% of growth inhibition.
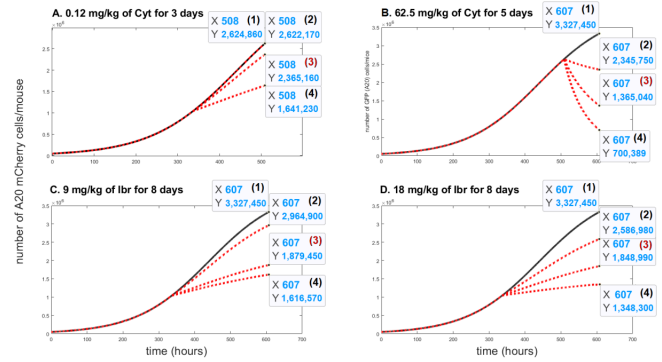
Figure 4. Evolution of the system in the absence of treatment (black lines) and with different choices for μ_{Ac}, in the context of every treatment protocol

- Ibr Low has a target cell growth inhibition percentage of 43.5%. This is best reached by using $\mu_{Ac} = 0.0041$, that provided 43.4% of growth inhibition.

- Ibr High has a target cell growth inhibition percentage of 44.5%. This is best reached by using $\mu_{Ac} = 0.0042$, that provided 44% of growth inhibition.

Concentration of Drugs (mg/kg)	Cell Growth Inhibition (%) from the Simulation Data	Cell Growth Inhibition (%) from the Experiment Data
Cyt 0.12	10	9
Cyt 62.5	59	58
Ibr 9	43.4	43.5
Ibr 18	44	44.5

Figure 5. Comparision between the experimental cell growth inhibition percentages and the simulated ones, obtained by fine tuning μ_{Ac} for each protocol

3.4 Simulation of a combined therapy

The last simulation performed by the authors had the goal of estimating the *simulated cell growth inhibition percentage* of a treatment comprising both Cytarabine (Cyt) and Ibrutinib (Ibr). The authors were able to simulate a combined therapy without modifying the system of equations (which, in principle, is built to model the injections of a single type of drug) by modyfing the initial conditions and the parameters of the model so that the combined therapy could be simulated as a single treatment (Fig. 6). In particular, the mixed treatment was obtained by combining Cyt High (62.5 mg/Kg of Cyt, $3 \cdot 10^{18}$ molecules of Cyt at each administration) and Ibr Low (9 mg/Kg of Ibr, $2.5 \cdot 10^{17}$ molecules of Ibr at each administration) for 8 days of treatment (5 days of treatment, 2 days of break, and another 3 days of treatment). This means injecting a total of $3.25 \cdot 10^{18}$ molecules at each administration. Since under these conditions Cyt represents approximately 92% of the total molecules, the combined treatment was parameterized by setting $\mu_C = (0.231 \cdot 0.92 + 0.116 \cdot 0.08) = 0.221$ and $\mu_{AC} = 0.012 + 0.0041 = 0.0161$. The simulation run with these parameters predicted a 95% cell growth inhibition.
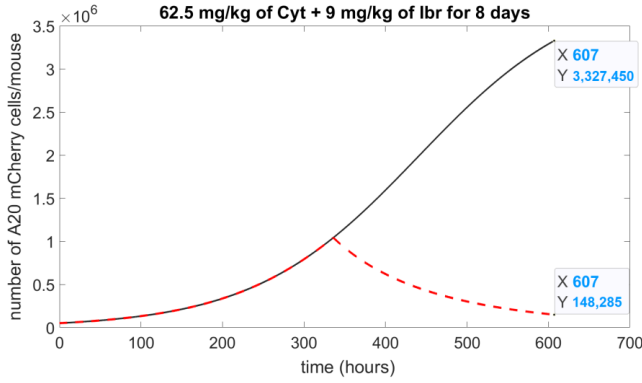
Figure 6. Evolution of the system in the absence of treatment (black line) and with a combined protocol (red line)

4. MATLAB simulations

4.1 Implementation

The deterministic simulations presented in the paper were replicated by using the MATLAB suite `ode45`. This library, dedicated to solve systems of differential equations in the form $y' = f(t, y)$, implemnts an adaptive-step Runge-Kutta integration algorithm of the fourth-order. A MATLAB script to solve the system of equation (1), (2), (3) for each treatment condition was developed and reported in a GitHub repository dedicated to this project [10].

The `simulations` folder contains the scripts used to run the simulation of our ODE system and the scripts used to plot the results. The folder `sim_data` contains the simulation results in form of CSV files, whose column represent: time, number of cancer cells, number of effector cells, number of drug molecules. The file names indicate the conditions, i.e.

- No treatment

- Cyt_high: Cyt 62.5mg/kg 3 days

- Cyt_low: Cyt 0.12mg/kg 5 days

- Ibr_high: Ibr 9mg/kg days 1-5 and 8-10

- Ibr_low: Ibr 18mg/kg days 1-5 and 8-10

- Cyt_Ibr: Cyt 62.5+ Ibr 9mg/kg days 1-5 and 8-10

These were taken directly from the paper. The folder `figures` contains the plots of the CSV files obtained using the script `plotter.py` found in the main folder.

4.2 Scripts

4.2.1 `model_no_trt.m`

This script contains a simplified model without treatment, simulated with initial conditions $A = 1000, E = 3.5 \cdot 10^5$. As expected given the instability of the tumor - free equilibrium, the number of A20 malignant cells rapidly grows to carrying capacity.

4.2.2 `model_trt.m`

The script at issue contains the final model of ODEs, and has been used to reproduce the 5 treatment protocols tested by the authors of the paper. The options for the numerical solution of the model are: `'MaxStep'`=1 to avoid that the integration skips a treatment. `'RelTol' = 1e-2` and `'AbsTol' = 1e-4` to avoid numerical errors due to the abrupt change in the number of drug molecules when a treatment is performed. To reproduce the behaviour of the shifted dirac-delta function found in equation (3) we used a conditional statement that checks, in between specific intervals, if the actual time is a multiple of τ (i.e., the time between two shots). If this condition holds, an amount of drug d is added to the system. Otherwise, the number of drug molecules is allowed to decrease.

The parameters for the equation were taken from the reference paper, whereas the parameters for the integration algorithm were adjusted in order to deal with the simulation of the treatments. In particular, the maximum step allowed was set to 1 hour to prevent the integrator to *skip* some treatments, and the tolerance was increased to avoid errors due to the abrupt increase in the number of drug molecules in correspondence to the delivery of treatments.

As it is, the script simulates the behaviour of the system in the presence of the mixed treatment Cyt_Ibr. However, to simulate the other protocols we just need to change the value of the parameter μ_{AC} and d, and additionally to modify the times in the conditional statements, in order to reflect the characteristics and requirements of each particualr treatment.

When reproducing the computations concerning the number of molecules per dose d for the different treatment protocols, we noticed that they did not match the results obtained by the authors of the paper: in particualr, the values reported in the paper were a thousand times smaller than the correct results. We decided to perform simulations both with the reported value $d \sim 10^{15}$ and the correct value $d \sim 10^{18}$. The plots obtained using the latter are reported below, for each treatment protocol, while the plots obtained with $d \sim 10^{15}$ can be examined in the `figures` folder, and have been labelled with the suffix `_1e15drug`.

Additionally, we noticed that the mathematical model does not take into account the natural production of effector cells: the second equation of the system admits a positive term only in the context of the recruitment effect carried out by the malignant cells on the immune population, without considering any other positive contributions. For this reason, we run additional simulations adding to equation (2) a term e_0 accounting for the natural production of effector cells. This parameter was derived form ref [36] of the main paper. The results of this set of simulations can be examined in the `figures` folder.

From the results of the various simulations we calculated the percentage growth inhibition of each group compared to the control group two days after the end of the treatment as:

$$G.I. = 1 - \frac{A_t}{A_{nt}}$$

Where A_t is the number of cancer cells in the treated group

28 hours after the end of the treatment and A_{nt} is the number of cancer cells in the control at the same time. The values we obtained are reported in Table 1, alongside the values reported in the main paper.

4.2.3 `model_cyt_infusion.m`
The third equation of the mathemtical model introduced in the previous sections assumes that, independently from the drug, each treatment is administered by τ - interposed injections. However, as discussed in section 2.1.2, Cytarabine has to be delivered though a continuous infusion. We thus decided to build a new mathematical model, able to describe a constant intake of Cytarabine, by adapting the treatment protocols reported in [7]. The modified system of equations can be appreciated in the files `model_cyt_infusion_high.m` and `model_cyt_infusion_low.m`. The protocols are as follows:

- `Cyt_infusion_low`: Cyt 200 mg · 24h / m² for 7 consecutive days + 1000 mg · 3h / m² every 12 h for 6 days.

- `Cyt_infusion_high`: Cyt 1000 mg · 3h / m² every 12 h for 5 days + 2000 mg · 6h / m² every 12 h on days 12, 13, 15, 17.

To simulate these therapeutic regimes, we had to convert the doses from $[mg/m^2]$ of human surface area in $[molecules/mouse]$ according to standard guidelines [11] and to calculate the corresponding cytotoxicity rate μ_{AC}. The latter calculation was done using the line

$$\mu_{AC} = 0.00018 \cdot dose[mg \cdot h/kg] + 0.00098$$

Interpolating the two data points present in [12]. Then, we needed the number of molecules that enter the body at each time-step during the infusion, to estimate this we used the mean value of the time-step when the treatment are delivered, calculated by looking at the vectors of time produced in of some preliminary simulations. The results of these simulations can be examined in the `figures` folder, and have been labelled with the prefix `Cyt_infusion`.

4.3 Results
A tentative to reproduce the results obtained by the paper was done. From the results of the various simulations, the percentage growth inhibition was calculated with respect to the control group two days after the end of the treatment as

$$G.I. = 1 - \frac{A_t}{A_{nt}}$$

Where A_t is the number of cancer cells in the treated group 28 hours after the end of the treatment and A_{nt} is the number of cancer cells in the control at the same time. The values we obtained are reportes in Table 1, alongside the values reported in the main pater.

The discrepancy in the growth inhibition for the Cyt high group, that was calculated at the time-point corresponding to

Group	Growth Inhibition (%)	GI (paper)	GI (exp)
Cyt low	11	10.0	9.0
Cyt high	70	59.0	58.0
Ibr low	44	43.4	43.5
Ibr high	45	44.0	44.5
Cyt + Ibr	96	95.0	-
Cyt infusion low	93	-	-
Cyt infusion high	98	-	-

Table 1. Growth inhibition calculated 2 days after the end of the treatments, with respect to the control group in the same day

two days after the end of the treatments, is probably due to some inconsistencies in the main paper, in which it is not clear when such value was calculated.
The results of the simulations without treatments are identical to the ones reported (Figure A1 in the paper), and so is the growth inhibition due to the combined use of a low dose of Ibr and a high dose of Cyt for 8 days (figure 6 in the paper). However, there is a mismatch in what was obtained from this project in trying to reporuce figure A2 and the figure itself. In particular, the most striking difference is that the tumor-free period we obtained after the 30 days of combined treatment is much shorter.
Regarding the adaptation of a treatment protocol involving the delivery of Cyt through infusion, we took as reference the paper [7], in which Cyt is used to treat acute myeloid leukemia in humans. Doses where adjusted according to standard guidelines [11] in order to pass from humans to mice. It has to be noted that these treatments involved the combined use of Cyt and another drug, which parameters have not been found. Therefore, the simulations are restricted to a therapy regiment with Cyt only.

5. Conclusions
Cyt is a drug not currently used to treat CLL that is more cytotoxic to A20 cells *in vitro* than Ibr, which suggests a repurposing of this cancer drug. Indeed, this prediction was vindicated when tested in the animal model presented in this paper. A numerical simulation of the potential effect of Cyt plus Ibr on A20 cells predicted that such a combination could increase cytotoxicity and inhibit cancer cell growth by up to 95%. It would now be valuable to test this combined treatment *in vivo*, especially as these drugs have different modes of action. This model exhibits several stable states that depend on biologically related parameters: Analysis of stability shows that the free-tumor Eqm_0^* equilibrium is not stable, which means that if there are no more cancer cells and the treatment is stopped, the model is in equilibrium without growth, albeit unstable. This may also represent a state of cancer cell dormancy, an adaptive strategy used by cancer cells to overcome drug cytotoxicity. This stage may persist until complete metabolism of the drug, which would allow tumor

growth to recur. The fixed point Eqm_1^* is a stable equilibrium reached when the number of cancer cells reaches its maximum. The system is not stable at Eqm_2^* equilibrium with periodical chemotherapy, which is obtained when treatment is stopped before the cancer cells are completely removed. The step of calculating the growth rate of cancer cells *in vivo* has to be carried out for each type of cancer cell, and it's easier to perform for blood-borne cancers. Current models do not easily help personalized chemotherapy dosing, partially because tumor cell growth rates vary between patients. The validation of experimental model with simulations studies can aid in selecting an optimal range of dosages to test. Furthermore, the model can be used to simulate combination drug therapy: the model predicted that a combination of Cyt and Ibr would lead to about 95% killing of A20 cells. Such high rates of killing are not expected in clinical practice, mainly due to subsequent toxicities. This model allows to predict a potentially effective new combination of drugs. Further experiments in vivo may reveal that two drugs with different modes of action may have acceptable efficacy at a lower dosage.

References

1. A., B. J. Treatment of Chronic Lymphocytic Leukemia. *The New England Journal of Medicine* **383,** 460–473 (2020).

2. Ciril, R. & Emilio, M. Chronic Lymphocytic Leukemia. *The New England Journal of Medicine* **333,** 1052–1057 (1995).

3. A., X., A., A. & I., K. Immunoglobulin heavy variable (IGHV) genes and alleles: new entities, new names and implications for research and prognostication in chronic lymphocytic leukaemia. *Immunogenetics* **67,** 61–66 (2015).

4. F., C. & M., S. Ibrutinib: First Global Approval. *Drugs* **74,** 263–271 (2014).

5. Novero, A., Ravella, P. M., Chen, Y., Dous, G. & Liu, D. Ibrutinib for B cell malignancies. *Experimental Hematology & Oncology* **3** (2014).

6. *National Center for Biotechnology Information. "PubChem Compound Summary for CID 24821094, Ibrutinib" PubChem,* https://pubchem.ncbi.nlm.nih.gov/compound/Ibrutinib.. Accessed: January 20, 2023.

7. Löwenberg, B. *et al.* Cytarabine Dose for Acute Myeloid Leukemia. *The New England Journal of Medicine* **364,** 1027–1036 (2011).

8. A., F. & P., T. Cytarabine. *StatPearls Publishing* (2022).

9. D., R. N. & J., S. G. High-Dose Cytarabine (HD araC) in the Treatment of Leukemias: a Review. *Current Hematologic Malignancy Report* **8,** 141–148 (2013).

10. Guadagnin Pattaro, A., Plazzotta, G. & Zanon, A. *Network Modeling and Simulation Project GitHub Repository* https://github.com/alessiagp/NetworkModProje 2023.

11. Nair, A. B. & Jacob, S. A simple practive guide for dose conversion between animals and human. *Journal of Basic Clinical Pharmaceutics* **7,** 27–31 (2016).

12. E., G. *et al.* Validation of a Mathematical Model Describing the Dynamics of Chemotherapy for Chronic Lymphocytic Leukemia In Vivo. *Cells* **11** (2022).